Cell Cycle Regulation of Tubulin RNA Level, Tubulin Protein Synthesis, and Assembly of Microtubules in *Physarum*

TIM SCHEDL, TIMOTHY G. BURLAND, KEITH GULL, and WILLIAM F. DOVE
McArdle Laboratory, University of Wisconsin, Madison, Wisconsin 53706. Dr. Gull's permanent address is Biological Laboratories, University of Kent, Canterbury, United Kingdom.

ABSTRACT The temporal relationship between tubulin expression and the assembly of the mitotic spindle microtubules has been investigated during the naturally synchronous cell cycle of the *Physarum* plasmodium. The cell cycle behavior of the tubulin isoforms was examined by two-dimensional gel electrophoresis of proteins labeled in vivo and by translation of RNA in vitro. α1-, α2-, β1-, and β2-tubulin synthesis increases coordinately until metaphase, and then falls, with β2 falling more rapidly than β1. Nucleic acid hybridization demonstrated that α- and β-tubulin RNAs accumulate coordinately during G2, peaking at metaphase. Quantitative analysis demonstrated that α-tubulin RNA increases with apparent exponential kinetics, peaking with an increase over the basal level of >40-fold. After metaphase, tubulin RNA levels fall exponentially, with a short half-life (19 min). Electron microscopic analysis of the plasmodium showed that the accumulation of tubulin RNA begins long before the polymerization of mitotic spindle microtubules. By contrast, the decay of tubulin RNA after metaphase coincides with the depolymerization of the spindle microtubules.

How is the execution of an event in the cell cycle related to the synthesis of the macromolecules that participate in the event? Successful execution of the cell cycle event mitosis depends on the proper functioning of the mitotic spindle. The major macromolecular components of the mitotic spindle are microtubules. Microtubules are formed by polymerization of tubulin "protomers," the protomer being comprised of one α- and one β-tubulin polypeptide (31). How is the synthesis of tubulin polypeptides regulated in relation to mitosis? Fulton and Simpson (21) have proposed that the pool of tubulin protomers used for mitosis is presynthesized. This is consistent with cytological observations of tissue culture cells, where, before polymerization of the mitotic spindle microtubules during prophase, the cytoplasmic microtubules disassemble (54). Biochemical support for a presynthesized pool is found in HeLa cells, where α- and β-tubulin polypeptides are synthesized throughout the cell cycle (6), and where equivalent amounts of total or polymerizable tubulin can be isolated from mitotic or log-phase cells (7). However, Bravo and Celis (6) do note a twofold increase in tubulin protein synthesis during mitosis. During the cell cycle of synchronized *Chlamydomonas*, there is an increase in tubulin protein synthesis that is controlled by an eightfold increase in α- and β-tubulin RNA level (1). Although this increased tubulin expression occurs during mitosis, it is also concurrent with regeneration of the flagellum. Thus in tissue culture cells and *Chlamydomonas*, examination of the relationship between tubulin synthesis and mitosis is complicated by the fact that tubulin also functions in cytoplasmic or flagellar microtubules.

In the multinucleate plasmodium of *Physarum*, cytoplasmic (or flagellar) microtubules have never been observed despite extensive searches by electron microscopy and indirect immunofluorescence microscopy with anti-tubulin antibodies (23). Microtubules have been observed only within the nucleus during the closed, naturally synchronous mitosis. Thus, *Physarum* is well suited for a direct study of the relationship between tubulin synthesis and mitosis. Pulse labeling of plasmodial proteins and resolution by two-dimensional gel electrophoresis has shown two polypeptides that are preferentially synthesized during late G2 phase of the cell cycle (27, 51). Initially, one polypeptide was identified as α-tubulin and another as β-tubulin (10). More recently, Burland et al. (8) have found that two α-tubulins (α1 and α2) and two β-tubulins (β1 and β2) are expressed in the plasmodium.

This study examines whether synthesis of all four tubulin isoforms in *Physarum* is coordinately regulated during the cell cycle, and how the synthesis is temporally related to the assembly and disassembly of the mitotic spindle. In addition, quantitation of tubulin RNA level over the cell cycle is

THE JOURNAL OF CELL BIOLOGY · VOLUME 99 JULY 1984 155-165

reported. Because it is feasible to grow large plasmodia that retain the natural mitotic synchrony, it was possible to examine tubulin protein synthesis, the organization of microtubules, and the level of tubulin RNA at multiple time points during the cell cycle of a single plasmodium.

MATERIALS AND METHODS

Physarum Plasmodial Strains: Diploid natural isolate Wis 1 (18) was used to isolate RNA for complementary DNA cloning. Inbred diploid [CLdxLU862] (16, 19) was used for all other experiments.

Bacterial Plasmids: The following plasmids were generous gifts: chick α- and β-tubulin complementary DNA (cDNA) clones pT1 and pT2 from D. Cleveland (12), *Drosophila* α- and β-tubulin genomic clones DTA4 and DTB4 from J. Natzle (46), and *Drosophila* actin genomic clone derived from λDmA2 from E. Fyrberg (22). Plasmid DNA was isolated by the method of Clewell (15).

Construction of cDNA Clones: cDNA clones were constructed by a modification of the second-strand priming method of Land et al. (29). Poly A-containing RNA, enriched by poly U Sepharose (Pharmacia Fine Chemicals, Piscataway, NJ) chromatography from RNA isolated from late G2 phase plasmodia (−15 min), was used as a template for reverse transcriptase (Life Sciences, Inc., St. Petersburg, FL). Sodium pyrophosphate (2 mM) was used instead of actinomycin D to inhibit anticomplementary strand synthesis (37). Tailing of the first strand, of double-stranded cDNA after S1 nuclease treatment, and of PstI-cut pBR322 was performed using terminal deoxyribonucleotidyl transferase (Ratliff Biochemicals, Los Alamos, NM) as described by Roewekamp and Firtel (44) except that $MnCl_2$ was used in place of $CoCl_2$. Competent *Escherichia coli* HB101 were transformed with annealed cDNA-pBR322 (17), and tetracycline-resistant colonies (25 μg/ml) were selected and then screened for ampicillin sensitivity (100 μg/ml).

About 1,000 colonies were screened by differential colony hybridization (49). Replicate filters were hybridized with ^{32}P-labeled, oligo dT-primed cDNA (45) synthesized either from late G2 phase RNA (−15 min) or from late reconstruction RNA (+ 90 min) templates. The vast majority of colonies showed hybridization signals of equal intensity for the two different cell cycle probes. For 40 colonies that showed possible differential hybridization, plasmid DNAs were purified (4), digested with PstI, electrophoresed in 1% agarose gels (33), transferred to nitrocellulose paper (48), and hybridized with chick or *Drosophila* α- or β-tubulin sequences ^{32}P-labeled by nick-translation (41). One colony identified by preferential hybridization to the late G2 phase cDNA probe contained a 1,400 base-pair (bp) insert homologous to both the chick and *Drosophila* α-tubulin clones (Ppc-α125). Two additional clones discussed in this report showed equal hybridization to late G2 and late reconstruction cDNA probes: Ppc-16 has a 670 bp insert homologous to an 850 base RNA, and Ppc-42 has a 1,600 bp insert homologous to a 3,800 base RNA.

Culture Methods: A single plasmodium was used for each complete cell cycle experiment. Petri dish-sized plasmodia (7-cm diam) were prepared without starvation as described by Burland et al. (8) and grown on mycological medium, the complex medium described by Turnock et al. (51).

To isolate 1–2-mg quantities of RNA from each of a number of time points during the cell cycle of a single plasmodium, it was necessary to use a preparative scale plasmodium (20–25-cm diam). Preparative plasmodia were grown at 26°C in a covered stainless steel tray, 45 cm square. Medium was circulated through the culture tray at 2.4 liters/h, at a depth of 12 mm, from a temperature-controlled reservoir (5 liters total volume in system). Exponentially growing microplasmodia (5–10 ml of 70% vol/vol microplasmodia in mycological medium, concentrated by centrifugation) were inoculated onto a dry filter in a ring pattern ~11 cm inside and 15 cm outside diameter. When excess medium had soaked into the filter, the plasmodium and supporting filter were transferred to the preequilibrated culture tray. In the tray, the plasmodium rested on a second filter supported by a perforated steel sheet; this served to hold the plasmodium just above the level of the medium, while the pair of filters ensured even contact between the medium and the plasmodium. The second synchronous mitosis (metaphase II, MII) occurred ~20 h after inoculation.

Polypeptide Labeling and Two-dimensional Gel Electrophoresis: At different times during the cell cycle, 7-mm disks were removed from the plasmodium and pulse-labeled with [^{35}S]methionine for 15 or 20 min as described by Burland et al. (8). For one cell cycle experiment, a more efficient labeling protocol was employed: plasmodial disks were placed on top of 10 μl (100 μCi) of [^{35}S]methionine for 20 min. Sample preparations for two-dimensional gels, gel electrophoresis, silver staining, and fluorography were performed as previously described (8) with the following modification: for preparative plasmodial samples, after lysis and nuclease treatment, an additional 100 μl of sample buffer was added.

RNA from different cell cycle samples was translated in vitro using the wheat germ cell-free system (43) as described by Boston et al. (5).

Microscopy: Progression of the cell cycle and synchrony across the plasmodium during an experiment was judged by ethanol-fixed smears observed by phase-contrast microscopy.

Electron microscopy was used to determine unambiguously the cell cycle stage and to assess whether microtubules were present or absent. Small pieces (1 mm^3) of plasmodium were fixed in 2% glutaraldehyde, 0.1 M PIPES (pH 6.8), 1 mM EGTA, 1 mM $MgSO_4$ for 1 h at room temp. After postfixation in 1% OsO_4 for 1 h, samples were dehydrated through a graded ethanol series and transferred to propylene oxide. Samples were embedded in Epon/Araldite and silver sections cut on a Porter-Blum MT-2 ultramicrotome (Sorval, Norwalk, CT) stained with uranyl acetate and lead citrate, and viewed at 75 kV in a Hitachi H-500 electron microscope (Hitachi, Ltd., Tokyo, Japan). The stages of mitosis are more accurately determined by electron than by phase microscopy.

RNA Isolation: At different times during the cell cycle, a sector-shaped sample (~25°, 12 cm in radius) with support filter was removed from a preparative plasmodium with a scalpel. From this piece, 7-mm disks were removed for protein labeling and smaller samples were removed for ethanol-fixed smears and for fixation for electron microscopy. The remaining piece of plasmodium (0.5–1.0 g wet wt) was lysed in 5.0 M guanidinium thiocyanate with a Polytron (Brinkmann Instruments Inc., Westbury, NJ), and RNA was purified away from DNA and polysaccharides by ultracentrifugation through CsCl (8). The RNA concentration was determined by optical density.

Hybridization Probes: For RNA quantitation, DNA restriction fragments containing homologous sequences were purified away from vector sequences by a modification of the method of Moran et al. (36), then labeled by nick-translation (41) with [^{32}P]dTTP or [^{32}P]dCTP (3,000 Ci/mmol; Amersham Corp., Arlington Heights, IL) to specific activities of $1–5 \times 10^8$ cpm/μg.

The *Physarum* α-tubulin probe was an internal 1 kilobase (kb) BglII-SacI fragment of cDNA clone Ppc-α125. The β-tubulin probe was either a 950-bp BglII-StuI fragment of chick cDNA clone pT2 (53) or a 2.35-kb EcoRI-BglI fragment from *Drosophila* clone DTB4 (46). The actin probe was a 1.8-kb HindIII fragment from *Drosophila* clone λDma2 (22). Probes Ppc-16 and Ppc-42 were excised PstI inserts of the respective cDNA clones. After labeling, probes were purified by phenol extraction, Sephadex G-75 chromatography, and filtration (Acrodisc, 0.45 μm; Gelman Sciences, Inc. Ann Arbor, MI).

Hybrid-selection assays demonstrate that the *Drosophila* actin probe hybridizes to *Physarum* actin RNA and that chick and *Drosophila* β-tubulin probes hybridize to β-tubulin RNA (8). Under the conditions used, the chick and *Drosophila* β-tubulin probes do not cross-hybridize with *Physarum* α-tubulin sequences (Schedl, T., unpublished observations).

RNA Quantitation: The relative levels of different RNA species from a series of cell cycle samples were quantitated by dot blotting (Fig. 1). Filters were prehybridized overnight at 42°C in 5XSSC (1XSSC is 15 mM sodium citrate, 150 mM NaCl), 200 μg/ml sonicated *E. coli* DNA, 200 μg/ml yeast transfer RNA, 100 μg/ml poly riboadenylic acid, 1 mg/ml polyvinylpyrrolidone, 1 mg/ml Ficoll, 50 mM sodium phosphate buffer (pH 7.0), 8 mM EDTA, 0.5% sodium dodecyl sulfate, and 10% Dextran sulfate (Pharmacia Fine Chemicals, Piscataway, NJ) in sealed plastic bags. The prehybridization solution was removed and an identical solution plus 0.12–0.6 μg of denatured, nick-translated probe was added and hybridized at 65°C for 6 h. Filters were washed in a vast excess of 1XSSC, 0.1% sodium dodecyl phosphate at 55°C for 2 h with agitation, except that filters hybridized with the β-tubulin probes were washed with 3XSSC, 0.1% sodium dodecyl phosphate. Filters were exposed to XAR-5 film (Eastman Kodak Co., Rochester, NY) using a Lightning-Plus intensifying screen (DuPont Instruments, Wilmington, DE).

Fig. 1, *a* and *b* shows autoradiograms of dot blots hybridized with the Ppc-α125 and chick β-tubulin probes. The autoradiograms were used as a template to cut out radioactive dots from which the number of counts per minute hybridized was determined by scintillation counting of filters in 4a20 cocktail (RPI Corporation, Mount Prospect, IL). The amount of probe hybridized to alkali-treated sample or when pBR322 was used as a probe (20–30 cpm/dot) was subtracted from the signal obtained for each dot of the RNA dilution series. Pilot experiments under the above conditions showed that hybridization had not reached completion with respect to time and concentration, even though (*a*) the probe was in stoichiometric excess with respect to homologous RNA on the filter and (*b*) the time and concentration were sufficient for the probe in solution to achieve $>10 \times Cot_{1/2}$. Presumably failure to hybridize to completion was a result of concatenation of nick-translated DNA in solution to the filter-bound RNA (20). Nevertheless, there is a linear relationship between the quantity of RNA in a dot and the amount of probe hybridized, as demonstrated in Fig. 1, *c* and *d*. For each time point and probe, the relationship between the amount hybridized and the quantity of RNA/dot was assessed by linear

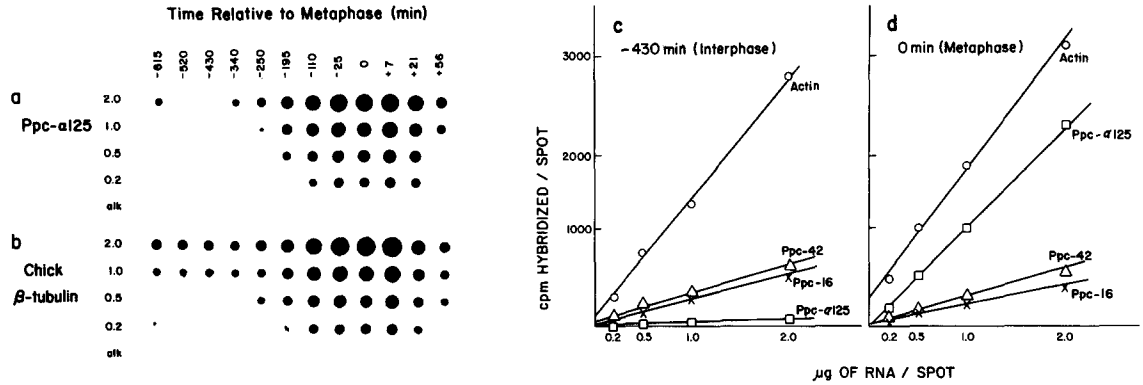

FIGURE 1 Quantitation of RNA levels by dot blot analysis. Autoradiograms of replicate dot blots hybridized with nick-translated probes (*a*) Ppc-α125, 4 h-exposure; and (*b*) chick β-tubulin; 2-wk exposure. Quantitation of RNA levels by the amount of probe hybridized to a titration series of RNA samples isolated at cell-cycle time points (*c*) −430 and (*d*) 0 min. Total RNA samples isolated at the indicated times during the cell cycle were diluted (2.0, 1.0, 0.5, and 0.2 μg, or 2 μg alkali treated), formaldehyde denatured (56), and bound to a series of replicate nitrocellulose filters with a 96-hole manifold apparatus (Bethesda Research Laboratories, Gaithersburg, MD). To avoid possible variable binding due to different amounts of *Physarum* RNA, all samples were adjusted to 10 μg with calf liver transfer RNA. Using ^{3}H-labeled SV40 complementary RNA (a gift of D. Reisman), >99% of the RNA was bound by this method. For each cell cycle experiment, a series of such filters were hybridized in duplicate with each probe. Radioactive dots were cut out and the number of counts per minute of probe hybridized was determined by liquid scintillation counting. Probe symbols: ○, actin; △, Ppc-42; ×, Ppc-16; and □, Ppc-α125. A linear relationship was obtained between the amount of probe hybridized and the number of micrograms of total *Physarum* RNA/dot. Lines were determined by linear regression analysis. The coefficient of variation between slopes of RNA titration curves from replicate dot blots was less than 17% for actin, 11% for Ppc-42, 25% for Ppc-16, and 13% for Ppc-α125. The slope of the line is a measure of the level of a given RNA (see Materials and Methods).

regression analysis using the computer program Minitab (Pennsylvania State University, University Park, PA). The relationship was consistent with a straight line whose intercept was the origin; in most cases R^2 was >95% and, using a *t* test, the intercept was not significantly different from zero at the 95% confidence level. Because the amount of probe hybridized was linearly dependent on the amount of homologous RNA in a given sample, the slope of the titration line determined by linear regression analysis can be used as a measure of the relative level of RNA at different time points. The slopes of the titration lines (Fig. 1, *c* and *d*) indicate that whereas actin, Ppc-16 and Ppc-42 RNA levels are similar, the Ppc-α125 RNA levels differ greatly in RNA isolated from −430 contrasted to 0-min cell cycle time points.

Northern Blot Analysis: 4 μg of total RNA from each time point were glyoxalated, run on 1.2 or 1.75% agarose gels (34), and transferred to Biodyne A nylon filters (1.2 μm, Pall Corp., Rosemont, IL) as described by Thomas (50). In some cases, dilutions of 2.0, 1.0, and 0.5 μg of total RNA were included. Hybridization, washing, and autoradiography were performed as described above. Radioactive bands were excised and the amount of probe hybridized was determined by liquid scintillation counting. Similar quantitative results were obtained using either Northern blot or dot blot methods.

RESULTS

Synthesis of All Four Tubulin Proteins Is Periodic during the Cell Cycle

The cell-cycle time of *Physarum* plasmodia under the conditions employed is 11–12 h. There is no G1; S phase begins immediately following metaphase and lasts 3 h; G2 occupies 7.5–8.5 h; and mitosis occupies ~30 min. To examine tubulin protein synthesis during the cell cycle, samples from a single plasmodium were pulse-labeled for 15 min with [^{35}S]methionine, and the labeled proteins were resolved by two-dimensional gel electrophoresis. To examine cell-cycle nuclear landmarks and assembly of the mitotic spindle, a sample was fixed for electron microscopy at the midpoint of each pulse. Samples were taken every 15 min from 195 min before metaphase until 120 min after metaphase. Fig. 2 shows examples of fluorographs of the two-dimensional gels and electron micrographs of representative nuclear morphologies from the midpoint of the corresponding pulse. The second synchronous metaphase (MII) after inoculation (see Materials and Methods) is defined as 0 min, with the indicated times (− before, + after metaphase) representing the time when the sample was fixed for electron microscopy. The identification of the tubulins and actin shown in two-dimensional gels (Figs. 2 and 4) has been described previously (8). Pulse-labeled time points shown in Fig. 2, *a–c* occur during interphase (see legends to Figs. 2 and 3 for a description of cell-cycle nuclear landmarks). Inspection of the fluorographs shows a coordinate increase in the labeling of α1-, α2-, β1-, and β2-tubulins from −165 to −60 min. Synthesis of all four tubulins during the earliest time points (−195 to −165) can be detected with longer exposures (see below). Labeling continues at a high rate until metaphase, and then decreases rapidly (Fig. 2, *d–f*). Fig. 2*d* shows a sample whose midpoint coincided with metaphase. At this point, tubulin labeling has begun to decrease. Fig. 2, *e* and *f* show labeling during an early (+15 min) and a later (+60 min) stage of nucleolar reconstruction. During the fall in tubulin protein synthesis after metaphase, the labeling of β2, and possibly of α2, decreases more rapidly than that of α1 and β1 (+ 15 min, Fig. 2*e*). Tubulin polypeptide labeling was never detected after the +30 min time point. In agreement with previous work (27, 51) actin, spot Z, and other non-tubulin proteins in the region of the gel were labeled continuously throughout the cell cycle.

The total levels of tubulin polypeptides over the cell cycle were analyzed by silver staining of two-dimensional gels. Qualitative inspection showed that all four tubulins were present throughout the cell cycle, even when they were not detected by pulse labeling (data not shown). This result, in concert with previous work (27, 51) indicates that the four tubulin species are stable. These results suggest that periodic

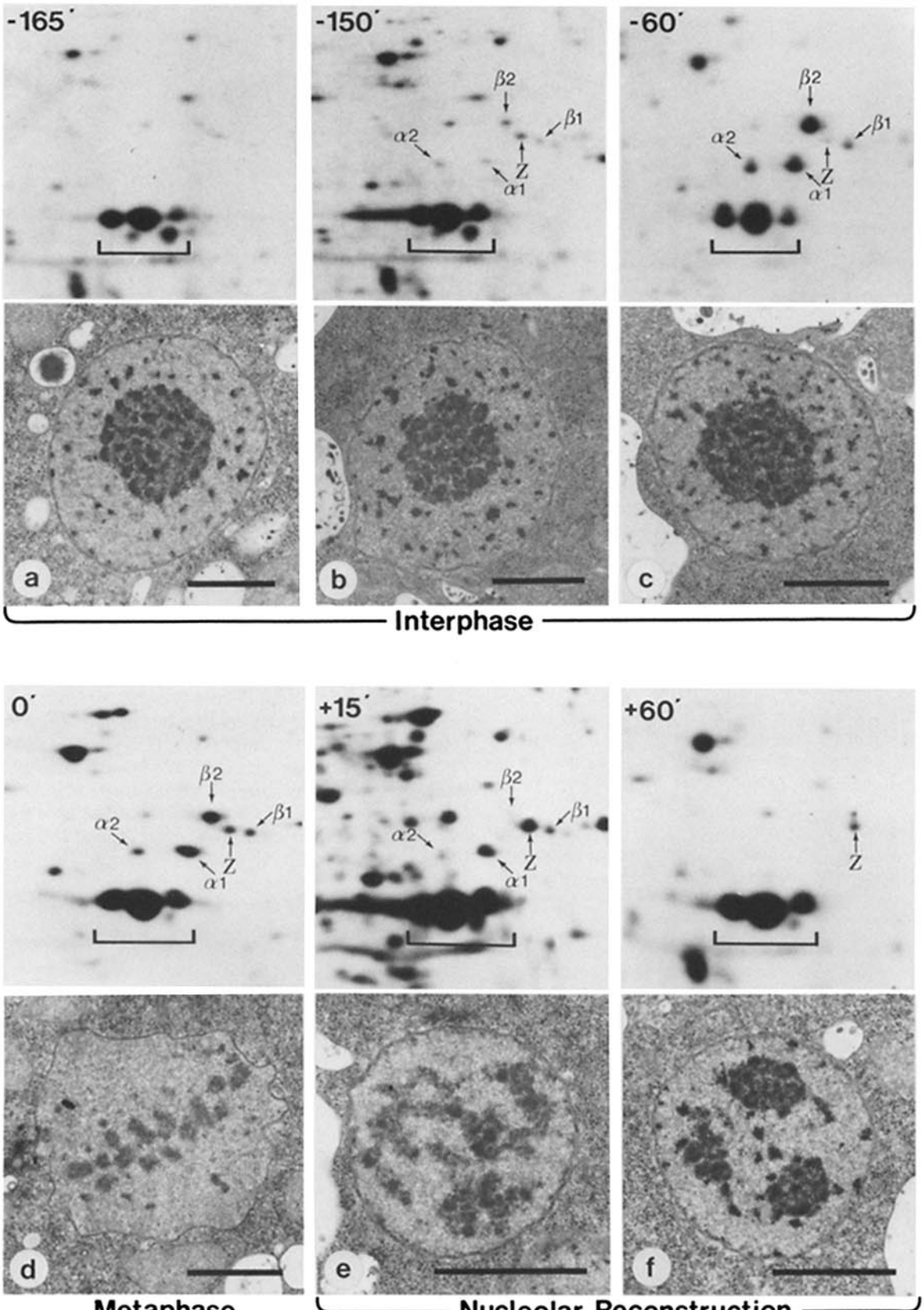
-165′
-150′
-60′
β2
β1
α2
Z
α1
a
b
c
Interphase
0′
+15′
+60′
d
e
f
Metaphase
Nucleolar Reconstruction

labeling is not the result of differential recovery or changes in stability of tubulins. Thus, changes in pulse labeling of tubulins probably reflect changes in the rate of protein synthesis.

Assembly of Microtubules during the Cell Cycle

To analyze the time of formation and the organization of microtubules over the cell cycle in the same plasmodium analyzed above, electron micrographs were examined at high magnification for characteristic 25-nm diam microtubules. Fig. 3 shows representative electron micrographs. Microtubules were first observed at −30 min (Fig. 3 *a*) in an otherwise interphase nucleus (*inset*). Microtubules were short, few in number, and reproducibly localized in one region of the nucleoplasm, to one side of the nucleolus. 15 min later (−15 min, Fig. 3 *b*) the cell cycle progressed to prophase (*inset* shows a typical prophase nucleus). The microtubules are in a starburst arrangement in the center of the nucleus, abutting the nucleolus. Microtubules became longer and more numerous. Fig. 3 *c* shows a longitudinal section through one pole of a metaphase nucleus such as that shown in Fig. 2 *d*. Long microtubules extend from the chromosomes, converge on the pole, and terminate before the nuclear envelope. No organized structure has yet been discerned at the pole, in contrast to the spindle pole body of *S. cerevisiae* (9). By 15 min after metaphase (Fig. 3 *d*), only rare, extremely short microtubules can be observed, randomly distributed throughout the nucleoplasm. Microtubules were never observed either in the cytoplasm or in nuclei, before −30 min, nor after +15 min. It is interesting to note that the first time that microtubules are observed (−30 min) corresponds to the point of nuclear commitment to mitosis in plasmodial cell cycle fusion experiments (52).

The data presented in Figs. 2 and 3 thus show that tubulin protein synthesis begins hours before microtubules can be detected by electron microscopy. By contrast, the fall in tubulin protein synthesis after metaphase is concurrent with disassembly of the mitotic spindle. To avoid depolymerization of microtubules during fixation for electron microscopy, fixation conditions that are known to preserve microtubules were employed (32). The ability to detect short, rare microtubules at +15 min strengthens the view that microtubules are largely absent over the remainder of the cell cycle. This conclusion is consistent with the absence of cytoplasmic microtubules throughout the cell cycle as judged by immunofluorescence microscopy (23). It should be noted that in this study, structures < ~100 nm in length could not be scored unequivocally as microtubules. Assuming an 8-nm diameter for an α-β-tubulin heterodimer (protomer) and 13 protofilaments per tubule (Gull, K., unpublished observation), the smallest microtubule likely to be scored would contain ~150 protomer units.

Tubulin Protein Synthesis Is Controlled by the Level of Translatable RNA

To determine the level of translatable RNAs for the two α- and two β-tubulins, total RNA was isolated from plasmodia before metaphase (−15 min) and after metaphase (+90 min). The RNA was translated in vitro and the polypeptide products were resolved on two-dimensional gels (see Materials and Methods). Before metaphase, translatable α1-, α2-, β1-, and β2-RNAs are abundant, whereas 90 min after metaphase translatable tubulin RNAs could not be detected (Fig. 4). Thus, for two cell-cycle time points, synthesis of all four tubulin species is coordinately regulated by the level of translatable RNA. A more detailed time course for translatable RNA is discussed below. Translatable RNA for actin, as well as for other proteins detected on the gel system, showed no variation between the −15 and +90 min time points.

The large change in levels of translatable tubulin RNA suggested a strategy for isolating tubulin cDNA clones. Complementary DNA clones were constructed using the −15 min RNA as a template (see Materials and Methods). These clones were then screened for differential hybridization (45) to ^{32}P-labeled cDNA probes synthesized from either −15 min or +90 min RNA templates. One clone that showed preferential hybridization to the pre-metaphase cDNA probe was also homologous to both the chick α-tubulin clone, pT1 (12), and the *Drosophila* α-tubulin clone, DTA4 (46, data not shown); it was named Ppc-α125. When Ppc-α125 DNA was used to hybrid-select translatable tubulin RNAs, it selected both α1 and α2 from the −15 min RNA (8). Thus Ppc-α125 is a *Physarum* (plasmodial) α-tubulin cDNA clone. Most of the cDNA clones did not show differential hybridization signals with the −15 and +90 min radioactive cDNA probes. Two of these clones (Ppc-16 and Ppc-42) were chosen as controls for RNA quantitation.

Changes in Tubulin RNA Levels during the Cell Cycle

To analyze the kinetics of α-tubulin RNA accumulation and its relationship to tubulin protein synthesis and micro-

FIGURE 2 Periodic tubulin protein synthesis and nuclear morphology during the cell cycle. At different times during the cell cycle, plasmodial samples were pulse-labeled with [^{35}S]methionine. Fluorographs of labeled polypeptides resolved by two-dimensional gels are in the upper panels: only the tubulin region is shown. Electron micrographs of samples fixed at the midpoint of the corresponding pulse-labeling are in the lower panels (see Materials and Methods for details). Two dimensional gels: isoelectric focusing is from left (basic) to right (acidic); sodium dodecyl sulfate electrophoresis is from top to bottom. Arrows indicate α1-, α2-, β1-, and β2-tubulins, nontubulin spot *Z*, the bracket indicates the actin region (8). Approximately 1 × 10^5 cpm was loaded per gel, although considerable variability in the amount of sample entering the gel was observed. However, using double-labeling techniques to correct for such variables, it has been shown that the rates of tubulin synthesis increase dramatically in late G2, whereas the rates of synthesis of most other proteins remains relatively constant (27, 51). Fluorography of time points −165, −150, and −60 min was 5 d, and for 0, + 15, and + 60 min, fluorography was 2 wk. The morphologies observed in low-magnification electron micrographs agree with previous work (28), showing that mitosis in the plasmodium is closed, with an anastral intranuclear spindle. Interphase nuclei *a*, *b*, and *c* show the characteristic electron-dense nucleolus with diffuse chromatin in the nucleoplasm. The metaphase nucleus *d* has condensed chromosomes aligned on the metaphase plate between two spindle poles, whereas the nuclear envelope, although irregularly shaped, remains intact. After metaphase the nuclei divide, chromatin decondenses, and the electron dense nucleolar material reappears and begins to coalesce into a single nucleolus (nucleolar reconstruction). Early and later stages of nucleolar reconstruction are shown in *e* and *f*, respectively. Bar, 2 μm. × 7,500–12,500.

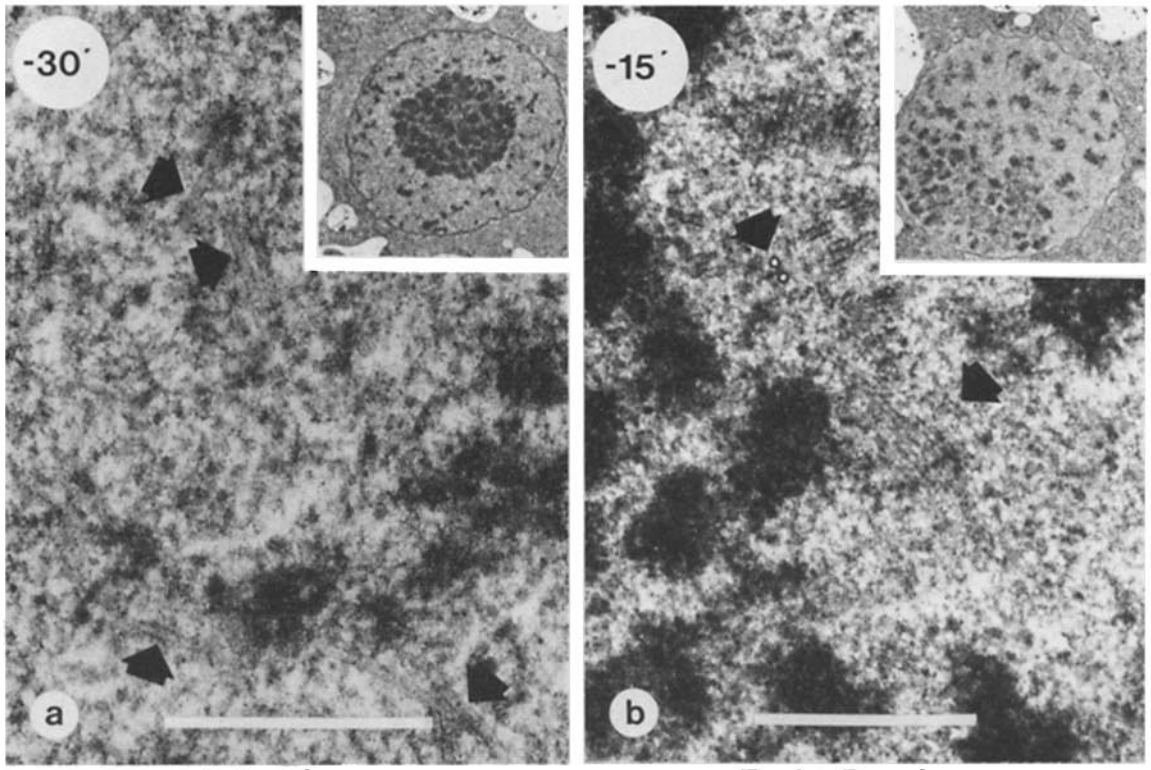

Interphase Early Prophase

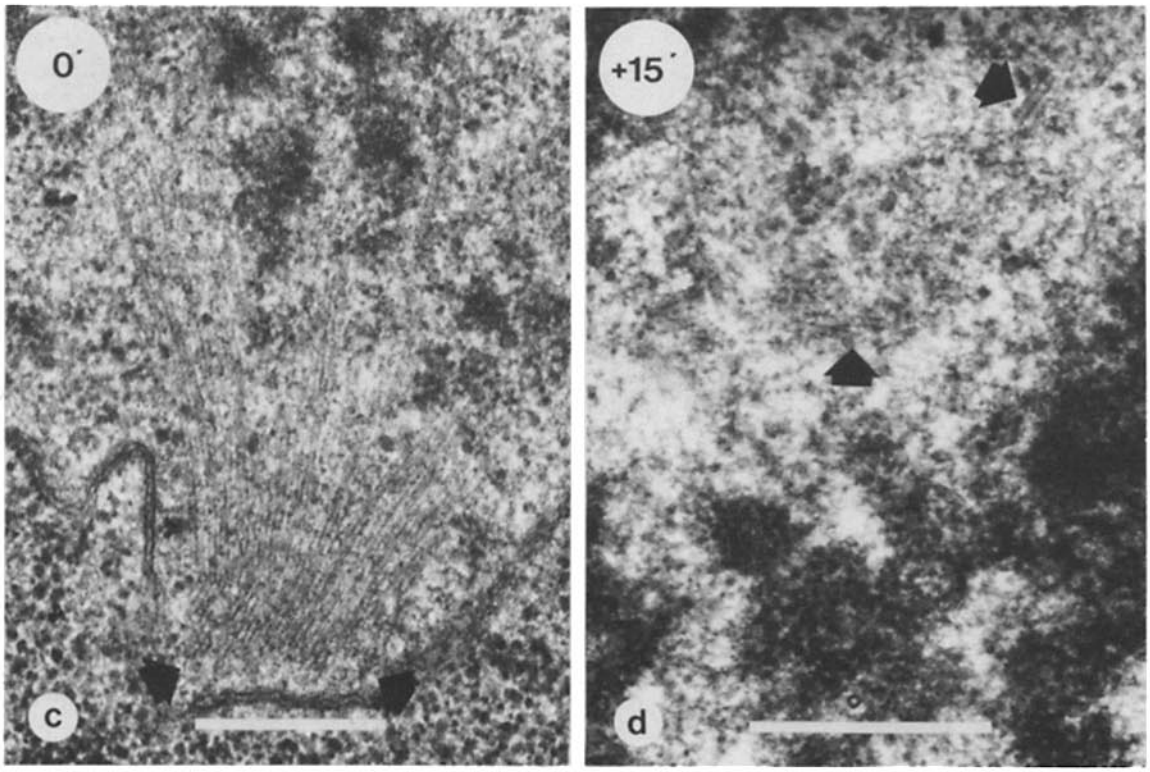

Metaphase Nucleolar Reconstruction

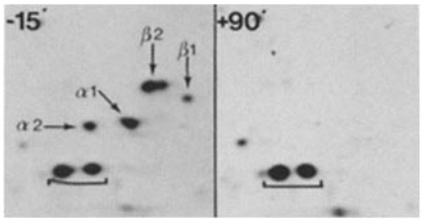

FIGURE 4 In vitro translation of RNAs isolated before and after metaphase. Total RNA (0.5 μg) isolated 15 min before or 90 min after metaphase was translated in a wheat germ extract with [^{35}S]-methionine; the labeled polypeptides were resolved on two-dimensional gels (see Materials and Methods). Arrows indicate α1-, α2-, β1-, and β2-tubulins; the actin polypeptides are bracketed.

tubule formation, samples were removed at different times in the cell cycle from a single preparative plasmodium. From each time point the following information was obtained: (*a*) protein synthesis was analyzed by pulse labeling with [^{35}S]-methionine; (*b*) cell cycle progression and the appearance and organization of microtubules was investigated by phase and electron microscopy; and (*c*) tubulin RNA levels were quantitated from total RNA isolated from the major part of each sample (see Materials and Methods). This complete analysis was performed twice, on independent preparative plasmodia. Although the cell cycle times differed (12 and 11 h), equivalent results were obtained. Data from one experiment are shown in Figs. 1 and 5, and data from the other in Fig. 6.

The relative levels of RNAs homologous to α-tubulin, actin, Ppc-42, and Ppc-16 probes were quantitated by dot blots as described in Materials and Methods and in Figs. 1 and 5. Actin, Ppc-42, and Ppc-16 were used as a control for the behavior of RNAs expected to be nonperiodic. Fig. 5, *a–c* show the levels of these RNAs, defined by the slope of the RNA titration curve, plotted as a function of the time during the cell cycle when the RNA sample were isolated; MII and MIII represent the second and third metaphases observed in the plasmodium after inoculation. The levels of actin, Ppc-42, and Ppc-16 RNAs vary by no more than a factor of two. Thus, within the resolution of the assay, actin, Ppc-42, and Ppc-16 RNAs represent a constant proportion of total RNA throughout the cell cycle. The behavior of actin RNA is consistent with the continuous synthesis of the actin polypeptides during the cell cycle.

Electron micrographs of the plasmodium at the peak of α-tubulin RNA accumulation (see below) showed a typical metaphase nuclear morphology (see Figs. 2 and 3). The sample isolated 25 min earlier had an early prophase morphology, whereas the sample isolated 7 min after metaphase had a very early stage of nucleolar reconstruction that follows telophase (data not shown). The time of appearance and the organization of microtubules agreed with results discussed earlier: microtubules were not observed before −30 or after +15 min (see Figs. 2 and 3).

The relative levels of α-tubulin RNA over the cell cycle are shown in Fig. 5*d*. To correct for variations due to sampling, each α-tubulin RNA level was normalized to that of actin, Ppc-42, or Ppc-16 RNA (see legend to Fig. 5). A low basal level of α-tubulin RNA, different from experimental background (see Fig. 1*c*), can be detected during late S phase and early G2. During G2, the level of α-tubulin RNA begins increasing with apparent exponential kinetics (doubling time of 79 min), reaching a maximum at metaphase. After metaphase, there is a rapid fall in RNA level, reaching the basal level before +140 min. At the metaphase peak, there is more than a 40-fold increase in α-tubulin RNA over the basal level. For at least the first 60 min after metaphase, α-tubulin RNA levels decay exponentially, with an apparent half-life of 19 min assuming that synthesis ceases after metaphase. The true half-life would be even less if some tubulin RNA continues to be synthesized postmetaphase.

Mitotic synchrony was assessed by fixing samples for microscopy simultaneously from opposite sides of the plasmodium (see Materials and Methods). No evidence of asynchrony was found, as judged by phase microscopy, for the plasmodium used in Figs. 1 and 5. The data presented in Fig. 6 were obtained from a plasmodium that showed asynchrony of ± 5 min as judged by electron microscopy. In neither case was there detectable asynchrony within a phase or electron microscope sample. Thus, the peak level of α-tubulin RNA occurred at metaphase to a resolution of 5 min.

Because the β-tubulin probes were heterospecific (chick or *Drosophila*), the hybridization signal was not sufficiently high for quantitation by scintillation counting. However autoradiograms of α- and β-tubulin dot blots (Fig. 1, *a* and *b*), show a qualitatively similar cell cycle pattern for β-tubulin RNA and α-tubulin RNA.

RNA levels were also quantitated by Northern blotting (see Materials and Methods). This method would permit detection of degraded RNA that may contribute significantly to the hybridization signal. The quantitative results from Northern blots were similar to those obtained by dot blots: actin, Ppc-16, and Ppc-42 RNAs represent a constant proportion of total RNA throughout the cell cycle; normalized α-tubulin RNA levels show a gradual increase peaking at metaphase, >40-fold over basal level, followed by a rapid exponential decay after metaphase (data not shown). Fig. 6 shows autoradiograms of Northern blots that illustrate this. Importantly, the Northern blots do not reveal any significant amount of RNA degradation (Fig. 6), even for the tubulin RNAs during the rapid decay after metaphase. However, both α- and β-tubulin RNAs do appear to show a slight decrease in size after

FIGURE 3 Assembly of microtubules during the cell cycle. Electron micrographs of microtubules within nuclei from the cell cycle experiment described in the text and Fig. 2. Insets show low-magnification nuclear morphologies for −30- and −15-min time points; nuclear morphologies for 0 and + 15 min are shown in Fig. 2*d* and e. (a) A few short microtubules (shown in longitudinal section, arrows) are first observed 30 min before metaphase, localized in one area of the nucleoplasm, to one side of the nucleolus, in an otherwise interphase nucleus. (*b*) At prophase (−15 min) microtubules (shown in cross- and longitudinal section, arrows) are in a starburst arrangement in the center of the nucleus, adjacent to the nucleolus. In the prophase nucleus *(inset)*, chromosomes are beginning to condense while the nuclear envelope remains intact. The nucleolus is acentric, appressed against the nuclear envelope and has begun to disperse. In the (c) metaphase nucleus, microtubules radiate from the spindle pole (arrows) across to the spindle equator. (*d*) By 15 min after metaphase, only a few short microtubules are seen, randomly distributed throughout the nucleoplasm. Bar, 500 nm. × 50,000–75,000.

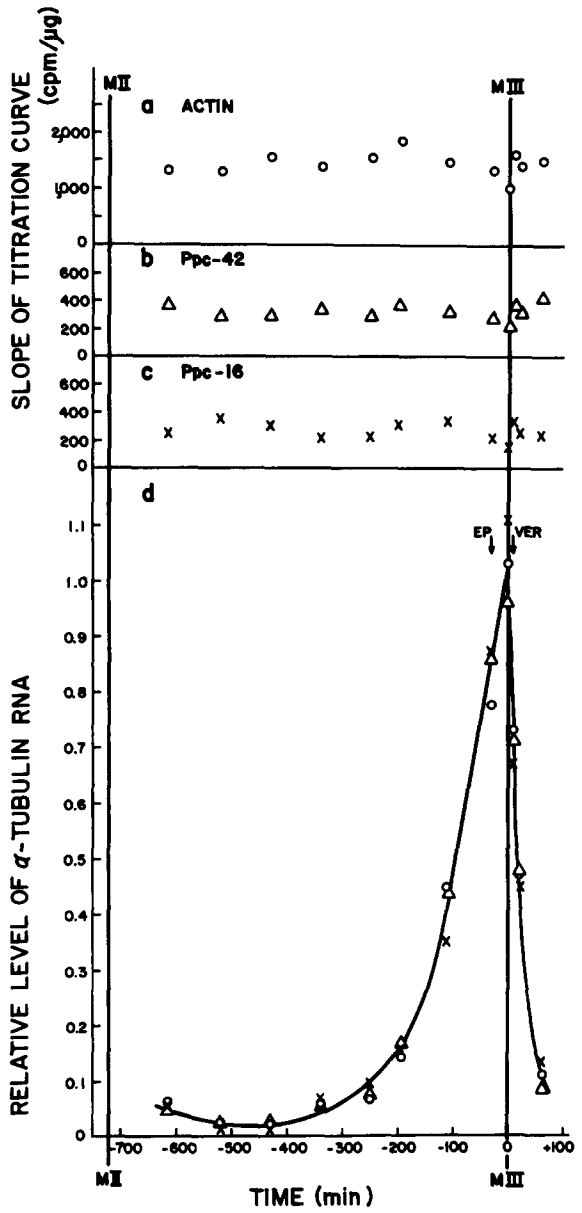

FIGURE 5 Levels of α-tubulin, actin, Ppc-42, and Ppc-16 RNAs during the cell cycle. Plot of RNA level vs. time in the cell cycle in reference to the third metaphase after inoculation (M III). The slope of the titration curve determined from dot blot analysis was used as a measure of RNA level (see Materials and Methods and Fig. 1). For (*a*) actin, (*b*) Ppc-42, and (*c*) Ppc-16, each point is the mean of slopes from duplicate dot blots. The α-tubulin RNA levels (*d*) have been normalized to correct for sampling errors. The mean α-tubulin slopes for a given point were divided by the mean of actin (○), Ppc-42 (△), or Ppc-16 (×) slopes from the same time point. To plot the normalized levels on the same scale, normalized α-tubulin levels were multiplied by the scaling factor (mean of all Ppc-42 or Ppc-16 slopes)/(mean of all actin slopes). Essentially equivalent results are obtained with each of these relative values. The minimum amplitude between peak and basal level was 42-fold from the α-tubulin RNA level normalized with Ppc-42. The exponential accumulation and decay constants for calculating RNA doubling time and half-life were determined by linear regression analysis of a plot $\log_e$ (relative RNA level) vs. time (data not shown). Note that hybridization efficiency can vary from experiment to experiment. This changes the number of counts per minute hybridized without affecting the linearity of the assay. Thus, the scale (relative level of α-tubulin RNA, [*d*]) will change without affecting the shape of the curve or quantitative conclusions, such as the ratio between peak and basal level, half-life, and doubling time.

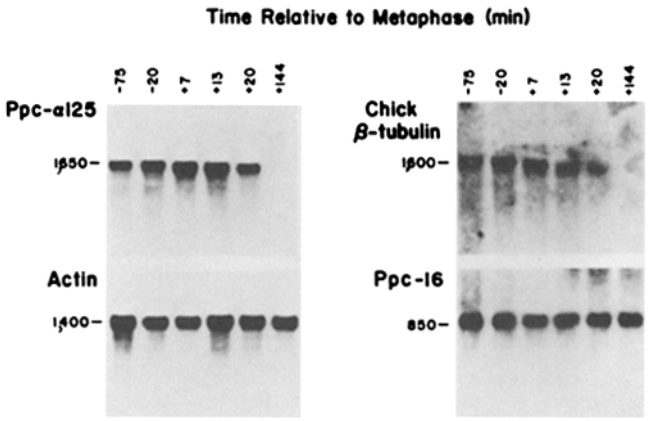

FIGURE 6 Northern blot analysis of α- and β-tubulin, actin, and Ppc-16 RNA during the cell cycle. Total RNA (4 μg) isolated at different times during the cell cycle was glyoxalated, electrophoresed on a 1.75% agarose gel, and transferred to Biodyne A paper. Replicate filters were hybridized with nick-translated Ppc-α125, chick β-tubulin, actin, or Ppc-16 probes (see Materials and Methods). Approximate molecular sizes in bases are given, determined from glyoxalated size markers RsaI or BglI digested pBR322 and 18*S* and 26*S* *Physarum* rRNAs. Exposures for Ppc-α125, actin, and Ppc-16 filters were 4 h; exposure for chicken β-tubulin was 2 wk.

metaphase, in contrast to actin and Ppc-16 RNAs. Although two α-tubulin and two β-tubulin RNAs have been inferred from in vitro translations (8, see below), only a single α-tubulin and a single β-tubulin RNA band was resolved by the gel system used. Because Ppc-α125 DNA can hybrid-select both α1- and α2-RNAs, the RNA levels quantitated by dot and Northern blot methods probably reflect the sum of α1- and α2-RNAs.

Is the observed level of total tubulin RNA proportional to the level of tubulin mRNA? The pattern of in vivo protein synthesis from preparative plasmodium time points agreed with the results presented earlier for a small plasmodium (Fig. 2 and data not shown). The earliest time that tubulin synthesis was detected in vivo in the preparative plasmodium was in a pulse label (20 min) starting at −280 min. Synthesis of α1, α2, β1, and β2 increased coordinately until metaphase. After metaphase, tubulin synthesis decreased until it was undetectable in time points after +30 min. The parallel kinetics of in vivo protein synthesis and total tubulin RNA levels suggests that the observed levels of tubulin RNA are proportional to the levels of mRNA in vivo.

In vitro translation of RNA isolated at different times during the cell cycle of the preparative plasmodia shows a similar pattern of protein synthesis as does in vivo labeling. In addition, after metaphase, translatable RNA for β2, and possibly for α2, decays more rapidly than those for β1- and α1-tubulin (data not shown). This agrees with the pattern of in vivo protein synthesis for the +15 min time point shown in Fig. 2*e*. The differential decay of translatable RNA for tubulin isoforms provides additional evidence that β1 and β2 must be encoded by different mRNAs.

DISCUSSION

The α1-, α2-, β1-, and β2-tubulins of the *Physarum* plasmodium are coordinately synthesized before and during their utilization in the assembly of the mitotic spindle microtubules. On disassembly of the spindle, synthesis of all the

isoforms falls, with $\beta 2$ falling more rapidly than $\beta 1$. This cell cycle pattern of tubulin protein synthesis is found both in vivo and by in vitro translation. The coordinated synthesis of the plasmodial tubulin isoforms may reflect the fact that all four are found in purified mitotic spindle preparations in the stoichiometry observed with in vivo and in vitro protein synthesis (Roobol, A., personal communication).

Nucleic acid hybridization demonstrated quantitatively (α-tubulin) and qualitatively (β-tubulin) a coordinate accumulation of tubulin RNAs in a peak pattern. The time course of total tubulin RNA levels parallels that of tubulin protein synthesis suggesting that the observed total RNA is proportional to amounts of messenger RNA. At least two events must occur during the cell cycle to produce this peak pattern: an event(s) during G2 that generates an exponential accumulation of α-tubulin RNA (doubling time of 79 min) peaking at metaphase, with a >40-fold increase in α-tubulin RNA over the basal level; and an event(s) at metaphase that generates exponential decay of α-tubulin RNA (apparent half-life of 19 min), reaching the basal level by mid-to-late S phase. The fall in α-tubulin RNA is about four times more rapid than the accumulation, with the apparent half-life representing <3% of the intermitotic time. This pattern of tubulin expression during the plasmodial cell cycle is observed under normal, unperturbed physiological conditions. The magnitude of the tubulin cell cycle periodicity in *Physarum* is far greater than that observed in HeLa cells, twofold (6), and *Chlamydomonas*, eightfold (1).

Levels of RNA are established by the rate of synthesis of the RNA and the rate of its degradation. Two general models can explain the peak pattern of tubulin RNA levels during the cell cycle. In the first model, tubulin RNA synthesis would be constant throughout the cell cycle and tubulin RNA levels would be determined solely by changes in RNA stability. Under this model, the constant rate of RNA synthesis must be at least that of the maximum observed rate of accumulation (steepest slope of curve before metaphase, Fig. 5*d*). However, to achieve the basal level of RNA observed after mitosis, a very short RNA half-life (<3 min) would be necessary. In the second class of model, RNA accumulation would involve changes in rates of synthesis, with RNA decay either constant or variable. Synthesis would cease at metaphase, and tubulin RNA would subsequently decay. The periodic accumulation of histone RNA during the yeast cell cycle provides an example where changes in both synthesis and stability regulate RNA levels (24, 25). The data in this report cannot distinguish between these two models for accumulation of tubulin RNA. Detailed analysis of the rates of synthesis and decay of *Physarum* tubulin RNAs may allow one to assess the relative contributions of synthesis and stability.

For either general model, the decay component must dominate after metaphase. Tubulin RNA may be intrinsically labile, with turnover observed only when there is no synthesis. Alternatively, degradation of tubulin RNA may be facilitated, for example by the increased pool of tubulin protomer created by disassembly of the mitotic spindle. Facilitated decay does seem to occur with yeast histone RNAs (25, 39), adenovirus early RNAs (2), and aggregation-specific RNAs in disaggregated *Dictyostelium* (35).

It is of interest to compare the cell-cycle expression and function of tubulin in *Physarum* with the cell-cycle expression and function of histones and homothallism endonuclease in yeast. Periodic expression of tubulins, histones (24, 25), and homothallism endonuclease (38) occurs before and during the utilization of these gene products in the cell cycle events mitosis, DNA synthesis, and mating type switching, respectively. Coordinate expression of the plasmodial tubulins ($\alpha 1$, $\alpha 2$, $\beta 1$, and $\beta 2$) and the yeast histones (H2A, H2B, H3, and H4; 25) occurs at the corresponding times in the cell cycle. However, whatever event(s) initiates the accumulation of tubulin RNA in *Physarum*, it is probably distinct from the G1 cell cycle regulation of histones and homothallism endonuclease expression. Histone and homothallism endonuclease expression is activated prior to initiation of DNA synthesis and may be related to the close proximity of origins of DNA replication to these genes (38, 40). By contrast, tubulin RNA accumulation begins after S phase. The behavior of the gene products in these three examples is also distinct. Functionally, the homothallism endonuclease is thought to be unstable, so that mating-type switching activity is limited during the cell cycle. By contrast, the *Physarum* tubulins are chemically stable. After assembly and disassembly of the mitotic spindle, the tubulin pool would seem to be available for reuse. This situation differs from that of histones, where there is not a free pool (42); the histones are irreversibly assembled into chromatin during their periodic synthesis.

It is not obvious what function is served by the periodicity of tubulin synthesis during the plasmodial cell cycle. Periodic tubulin synthesis may control spindle microtubule polymerization by raising the tubulin protomer pool to the concentration necessary for microtubule assembly. But, synthesis of tubulin alone seems not to be an adequate cause for the mitotic transition in that the pool of tubulin is as large just after mitosis as before mitosis. Synthesis of tubulin would become important for microtubule assembly if the tubulin protomer were modified, and lost function during a cycle of assembly and disassembly of the mitotic spindle. However, no modifications have been detected that alter the mobility of α- or β-tubulin spots in two-dimensional gels of plasmodial tubulins throughout the course of mitosis (unpublished observations). Determination of whether tubulin molecules synthesized during one cycle are utilized in that and subsequent cycles should be feasible in the *Physarum* plasmodium. It seems more plausible that assembly is controlled primarily by microtubule organizing centers, because they seem to show a cell cycle variation in competence to assemble microtubules (26, 47). Thus, the periodicity of tubulin synthesis does not, by itself, provide a simple explanation for the control of mitotic spindle assembly.

The event(s) that result in the fall of tubulin RNA levels after metaphase is temporally correlated with the depolymerization of the spindle microtubules. Treatment of cultured cells with antimitotic agents that depolymerize microtubules causes the cessation of α- and β-tubulin protein synthesis and a decrease in the steady-state levels of α- and β-tubulin RNA (3, 11, 13). To explain these observations, an autoregulatory model has been proposed in which the increased level of unpolymerized tubulin depresses tubulin synthesis (3, 13). Could this proposed autoregulation also be responsible for the decay of tubulin RNA after metaphase? Microtubules were not observed by electron microscopy before −30 min and later than +15 min. Based on the absence of microtubules, one assumes that all of the tubulin exists in the protomer form outside the short time interval from −30 to +15 min. This assumption would be incorrect if tubulin were polymerized into microtubules smaller than the limit of ob-

servation, or if a class of microtubules or other tubulin polymer exists that is undetectable, both under the conditions used for electron microscopy in this study, and under the conditions used for immunofluorescence microscopy by Havercroft and Gull (23). Because the tubulin proteins are chemically stable, synthesis will change their level by no more than two- to four-fold over the cell cycle. From ~−280 to −30 min, tubulin RNA level increases concurrently with increased level of tubulin protomer as a result of new protein synthesis without assembly into microtubules. Furthermore, at just before −30 min when tubulin RNA is accumulating, the unpolymerized tubulin pool must be almost as large as that at 15 min after metaphase, when tubulin RNA level is falling. Thus, if tubulin RNA is regulated by the size of the tubulin protomer pool as suggested by the autoregulatory model, this regulation must be sensitive to changes in the tubulin protomer pool of less than twofold. That such a small increase in tubulin protomer pool could depress tubulin expression is consistent with the observation that tubulin synthesis is suppressed when tubulin levels are elevated 25–50% by microinjection (14).

The complementary autoregulatory response would be to increase tubulin synthesis when the tubulin protomer pool is depleted. Evidence for such an increase in response to antimitotic agents that deplete the tubulin protomer pool has not been resolved (3, 13). Depletion of the tubulin pool seems not to underlie the induction of tubulin RNA accumulation during flagellar regeneration in *Chlamydomonas* (30, 55). In the *Physarum* plasmodium accumulation of tubulin RNA begins at least 250 min before microtubules are observed. Thus, the event(s) during G2 that initiates the exponential accumulation of tubulin RNA is clearly not a result of assembly of the mitotic spindle microtubules and seems unrelated to the behavior of the tubulin protomer pool.

We thank R. Boston who collaborated with us on some of the experiments, G. Turnock for advice on growing large plasmodia, L. Johnson for assistance with data analysis, Carol Sattler and Wanda Russell for assistance with electron microscopy, and Mary Jo Gilden for typing the manuscript. Our colleagues J. Ross, C. Gross, G. Borisy, L. Johnson, and L. Green gave helpful comments on the manuscript. Keith Gull was a recipient of the Pogonophora of Wisconsin Award.

Dr. Gull acknowledges financial support from SERC (United Kingdom) and a Wellcome Research Travel Grant. Our research was supported by Program Project Grant CA-23076 in Tumor Biology, Core Grant CA-07175, and Training Grant 5-T32-CA-09135 from the National Cancer Institute.

Received for publication 16 January 1984.

REFERENCES

1. Ares, M., and S. Howell. 1982. Cell cycle stage-specific accumulation of mRNAs encoding tubulin and other polypeptides in *Chlamydomonas*. *Proc. Natl. Acad. Sci. USA*. 79:5577–5581.
2. Babich, A., and J. R. Nevins. 1981. The stability of early adenovirus mRNAs is controlled by the viral 72 kd DNA-binding protein. *Cell*. 26:371–379.
3. Ben-Ze'ev, A., S. R. Farmer, and S. Penman. 1979. Mechanism of regulating tubulin synthesis in cultured mammalian cells. *Cell*. 17:319–325.
4. Birnboim, H. C., and J. Doly. 1979. A rapid alkaline extraction procedure for screening recombinant plasmid DNA. *Nucleic Acids Res.* 7:1513–1523.
5. Boston, R. S., T. J. Miller, J. E. Mertz, and R. R. Burgess. 1982. *In vitro* synthesis and processing of wheat α-amylase. *Plant Physiol.* 69:150–154.
6. Bravo, R., and J. E. Celis. 1980. A search for differential polypeptide synthesis throughout the cell cycle. *J. Cell Biol.* 84:795–802.
7. Bulinski, J. C., J. A. Rodriguez, and G. G. Borisy. 1980. Test of four possible mechanisms for the temporal control of spindle and cytoplasmic microtubule assembly in HeLa cells. *J. Biol. Chem.* 255:1684–1688.
8. Burland, T. G., K. Gull, T. Schedl, R. S. Boston, and W. F. Dove. 1983. Cell type-dependent expression of tubulins in *Physarum*. *J. Cell Biol.* 97:1852–1859.
9. Byers, B., and L. Goetsch. 1975. Behavior of spindles and spindle plaques in the cell cycle and conjugation of *Saccharomyces cerevisiae*. *J. Bacteriol.* 124:511–523.
10. Chang, M. T., W. F. Dove, and T. G. Laffler. 1983. The periodic synthesis of tubulin in the *Physarum* cell cycle. *J. Biol. Chem.* 258:1352–1356.
11. Cleveland, D. W., and J. C. Havercroft. 1983. Is apparent autoregulatory control of tubulin synthesis nontranscriptionally regulated? *J. Cell Biol.* 97:919–924.
12. Cleveland, D. W., M. A. Lopata, R. J. MacDonald, N. J. Cowan, W. J. Rutter, and M. W. Kirschner. 1980. Number and evolutionary conservation of α- and β-tubulin and cytoplasmic β- and α-actin genes using specific cloned cDNA probes. *Cell*. 20:95–105.
13. Cleveland, D. W., M. A. Lopata, P. Sherline, and M. W. Kirschner. 1981. Unpolymerized tubulin modulates the level of tubulin mRNAs. *Cell*. 25:537–546.
14. Cleveland, D. W., M. F. Pittenger, and J. R. Feramisco. 1983. Elevation of tubulin levels by microinjection suppresses new tubulin synthesis. *Nature (Lond.)*. 305:738–740.
15. Clewell, D. B. 1972. Nature of ColE1 plasmid replication of *E. coli* in the presence of chloramphenicol. *J. Bacteriol.* 110:667–676.
16. Cooke, D. J., and J. Dee. 1975. Methods for the isolation and analysis of plasmodial mutants in *Physarum polycephalum*. *Genet. Res.* 24:175–187.
17. Dagert, M., and S. D. Ehrlich. 1979. Prolonged incubation in calcium chloride improves the competence of *E. coli* cells. *Gene (Amst.)*. 6:23–28.
18. Dee, J. 1960. A mating-type system in an acellular slime mold. *Nature (Lond.)*. 185:780–781.
19. Dee, J. 1978. A gene unlinked to mating-type affecting crossing between strains of *Physarum polycephalum*. *Genet. Res.* 31:85–92.
20. Flavell, R. A., P. Borst, and E. J. Birfelder. 1974. DNA-DNA hybridization on nitrocellulose filters 2. concatenation effects. *Eur. J. Biochem.* 47:545–548.
21. Fulton, C., and P. A. Simpson. 1979. Tubulin pools, synthesis and utilization. *In* Microtubules. K. Roberts and J. S. Hyams, editors. Academic Press, Inc., New York. 65–116.
22. Fyrberg, E. A., K. L. Kindle, N. Davidson, and A. Sodja. 1980. The actin genes of *Drosophila:* a dispersed multigene family. *Cell*. 19:365–379.
23. Havercroft, J. C., and K. Gull. 1983. Demonstration of different patterns of microtubule organization in *Physarum polycephalum* myxamoebae and plasmodia using immunofluorescence microscopy. *Eur. J. Cell Biol.* 32:67–74.
24. Hereford, L. M., S. Bromley, and M. A. Osley. 1982. Periodic transcription of yeast histone genes. *Cell*. 30:305–310.
25. Hereford, L. M., M. A. Osley, J. R. Ludwig, and C. S. McLaughlin. 1981. Cell-cycle regulation of yeast histone mRNA. *Cell*. 24:367–375.
26. Kuriyama, R., and G. G. Borisy. 1981. Microtubule-nucleating activity of centrosomes in Chinese hamster ovary cells is independent of the centriole cycle but coupled to the mitotic cycle. *J. Cell Biol.* 91:822–826.
27. Laffler, T. G., M. T. Chang, and W. F. Dove. 1981. Periodic synthesis of microtubular proteins in the cell cycle of *Physarum*. *Proc. Natl. Acad. Sci. USA*. 78:5000–5004.
28. Lafontaine, J., and M. Cadrin. 1982. Nuclear organization during the cell cycle in the myxomycete *Physarum polycephalum*. *In* Cell Biology of *Physarum* and *Didymium*, Vol. 1. H. C. Aldrich and J. W. Daniel, editors. Academic Press, Inc., New York. 287–312.
29. Land, H., M. Grez, H. Hauser, W. Lindenmaier, and G. Schütz. 1981. 5′-terminal sequences of eucaryotic mRNA can be cloned with high efficiency. *Nucleic Acids Res.* 9:2251–2266.
30. Lefebvre, P. A., S. A. Nordstrom, J. E. Moulder, and J. L. Rosenbaum. 1978. Flagellar elongation and shortening in *Chlamydomonas*. IV. Effects of flagellar detachment, regeneration, and resorption on induction of flagellar protein synthesis. *J. Cell Biol.* 78:8–27.
31. Luduena, R. L. 1979. Biochemistry of tubulin. *In* Microtubules. K. Roberts and J. S. Hyams, editors. Academic Press, Inc., New York. 65–116.
32. Luftig, R., P. McMillan, J. Weatherbee, and R. Weihing. 1977. Increased visualization of microtubules by an improved fixation procedure. *J. Histochem. Cytochem.* 25:175–187.
33. McDonnell, M. W., M. N. Simon, and F. W. Studier. 1977. Analysis of restriction fragments of T7 DNA and determination of molecular weights by gel electrophoresis in neutral and alkaline gels. *J. Mol. Biol.* 110:119–146.
34. McMasters, G. K., and G. G. Carmichael. 1977. Analysis of single- and double-stranded nucleic acids on polyacrylamide and agarose gels by using glyoxal and acridine orange. *Proc. Natl. Acad. Sci. USA*. 74:4835–4838.
35. Mangiarotti, G., P. Lefebvre, and H. F. Lodish. 1982. Differences in the stability of developmentally regulated mRNAs in aggregated and disaggregated *Dictyostelium discoideum* cells. *Dev. Biol.* 89:82–91.
36. Moran, L., M. E. Mirault, A. Tissieres, J. Lis, P. Schedl, S. Artavanis-Tsakonas, and W. Gehring. 1979. Physical map of two *D. melanogaster* DNA sequences coding for the 70,000 dalton heat shock protein. *Cell*. 17:1–8.
37. Myers, J. C., and S. Spiegelman. 1978. Sodium pyrophosphate inhibition of RNA-DNA hybrid degradation by reverse transcriptase. *Proc. Natl. Acad. Sci. USA*. 75:5329–5333.
38. Nasmyth, K. 1983. Molecular analysis of cell lineage. *Nature (Lond.)*. 302:670–676.
39. Osley, M. A., and L. M. Hereford. 1981. Yeast histone genes show dosage compensation. *Cell*. 24:377–384.
40. Osley, M. A., and L. M. Hereford. 1982. Identification of a sequence responsible for periodic synthesis of yeast histone H2A mRNA. *Proc. Natl. Acad. Sci. USA*. 79:7689–7693.
41. Rigby, P. W., M. Dieckmann, C. Rhodes, and P. Berg. 1977. Labelling deoxyribonucleic acid to high specific activity *in vitro* by nick translation with DNA polymerase I. *J. Mol. Biol.* 113:237–251.
42. Riley, D., and H. Weintraub. 1979. Conservative segregation of parental histones during replication in the presence of cycloheximide. *Proc. Natl. Acad. Sci. USA*. 76:328–332.
43. Roberts, B. E., and B. M. Patterson. 1973. Efficient translation of tobacco mosaic virus RNA and rabbit globin 9S RNA in a cell-free system from commercial wheat germ. *Proc. Natl. Acad. Sci. USA*. 70:2330–2334.
44. Roewekamp, W., and R. A. Firtel. 1980. Isolation of developmentally regulated genes from *Dictyostelium*. *Dev. Biol.* 79:409–418.
45. St. John, T. P., and R. W. Davis. 1979. Isolation of galactose-inducible DNA sequences from *Saccharomyces cerevisiae* by differential plaque filter hybridization. *Cell*. 16:443–452.
46. Sanchez, F., J. E. Natzle, D. W. Cleveland, M. W. Kirschner, and B. J. McCarthy. 1980. A dispersed multigene family encoding tubulin in *Drosophila melanogaster*. *Cell*. 22:845–854.
47. Snyder, J. A., and J. R. McIntosh. 1975. Initiation and growth of microtubules from mitotic centers in lysed mammalian cells. *J. Cell Biol.* 67:744–760.
48. Southern, E. 1975. Detection of specific sequences among DNA fragments segregated by gel electrophoresis. *J. Mol. Biol.* 98:503–517.

49. Thayer, R. E. 1979. An improved method for detecting foreign DNA in plasmids of *E. coli*. *Anal. Biochem.* 98:60–63.
50. Thomas, P. S. 1980. Hybridization of denatured RNA and small DNA fragments transferred to nitrocellulose. *Proc. Natl. Acad. Sci. USA.* 77:5201–5205.
51. Turnock, G., J. Chambers, and B. Birch. 1981. Regulation of protein synthesis in the plasmodial phase of *Physarum polycephalum*. *Eur. J. Biochem.* 120:529–534.
52. Tyson, J. J. 1982. Periodic phenomena in *Physarum*. *In* Cell Biology of *Physarum* and *Didymium*, Vol. 1. H. C. Aldrich and J. W. Daniel, editors. Academic Press, Inc., New York. 61–101.
53. Valenzuela, P., M. Quiroga, J. Zaldivar, W. J. Rutter, M. W. Kirschner, and D. W. Cleveland. 1981. Nucleotide and corresponding amino acid sequences encoded by α-tubulin and β-tubulin mRNAs. *Nature (Lond.).* 289:650–655.
54. Weber, K. 1976. Visualization of tubulin-containing structures by immunofluorescence microscopy: cytoplasmic microtubules, mitotic figures and vinblastine induced paracrystals. *In* Cell Motility. R. Goldman, T. Pollard, and J. Rosenbaum, editors. Cold Spring Harbor Laboratory, Cold Spring Harbor, NY. 403–418.
55. Weeks, D., P. S. Collis, and M. Gealt. 1977. Control of induction of tubulin synthesis in *Chlamydomonas reinhardi*. *Nature (Lond.).* 268:667–668.
56. White, B. A., and F. C. Bancroft. 1982. Cytoplasmic dot hybridization. *J. Biol. Chem.* 257:8569–8572.